The first measurement of plasma density in an ECRIS-like device by means of a frequency-sweep microwave interferometer

D. Mascali,[1,a)] G. Torrisi,[1] O. Leonardi,[1] G. Sorbello,[1,2] G. Castro,[1] L. G. Celona,[1]
R. Miracoli,[3] R. Agnello,[1] and S. Gammino[1]
[1]*INFN - Laboratori Nazionali del Sud, 95123 Catania, Italy*
[2]*Universitá di Catania, Dipartimento di Ingegneria Elettrica Elettronica e Informatica, 95125 Catania, Italy*
[3]*ESS Bilbao, 48170 Zamudio, Spain*

The note presents the first plasma density measurements collected by a novel microwave interferometer in a compact Electron Cyclotron Resonance Ion Sources (ECRIS). The developed K-band (18.5 ÷ 26.5 GHz) microwave interferometry, based on the Frequency-Modulated Continuous-Wave method, has been able to discriminate the plasma signal from the spurious components due to the reflections at the plasma chamber walls, when working in the extreme unfavorable condition $\lambda_p \simeq L_p \simeq L_c$ (λ_p, L_p, and L_c being the probing signal wavelength, the plasma dimension and the plasma chamber length, respectively). The note describes the experimental procedure when probing a high density plasma ($n_e > 1 \cdot 10^{18}\,\mathrm{cm}^{-3}$) produced by an ECRIS prototype operating at 3.75 GHz.

I. INTRODUCTION

Interferometry is a non-intrusive way for measuring the line-averaged electron density of plasmas.[1] For density values in the range 10^{11}-10^{13} cm^{-3} (such as for plasmas of thermonuclear fusion reactors and/or heavy ion sources for accelerators), the probing beam wavelength λ_p lies in the range of few centimetres, that is—in case of ion sources—comparable to the plasma chamber radius L_c and to the plasma size L_p. This unfavorable $\lambda_{RF} \simeq L_p \simeq L_c$ condition causes the antenna-to-antenna signal being affected by superimposed contributions coming from reflections at the chamber walls. Therefore, the usual "Mach-Zehnder" scheme must be updated to the specific case, also changing the measurement technique and the post-processing procedure of the collected data. Hereinafter the first measurements obtained at Instituto Nazionale di Fisica Nucleare-Laboratori Nazionali del Sud (INFN-LNS) with the frequency-sweep interferometer named VESPRI (VEry Sensitive evaluation of Plasma density by micRowave Interferometry) are presented to complete the description of the technical design and the preliminary calibration phases already done in a previous work.[2]

II. THEORY AND EXPERIMENTAL METHOD

Fig. 1 illustrates the adopted scheme,[3] which is based on two conical-horn antennas launching into the plasma chamber a probing signal in the range 18.5–26.5 GHz. The signal is synthesized by a frequency-sweep oscillator. The superposition of the reference and plasma leg signals produces a beating such as $P_{M(t)} = \langle |M(t)|^2 \rangle = S(t) = 2A^2\cos^2\left(\frac{\phi_p + \phi_2 - \phi_1}{2}\right)$, where $\phi_1(\omega)$ denotes the phase shift due to the dispersion in the reference leg waveguide, $\phi_2(\omega)$ the one due to the waveguide dispersion in the plasma leg, $\phi_p(\omega)$ is due to the plasma, ω is the operating frequency, k_g is the wavenumber in the waveguide, ω_c is the waveguide cutoff frequency, and k_p is the wavenumber in the plasma (depending ω_p on the plasma frequency and so on the unknown electron density n_e). The time-dependent phase shift $\Delta\phi(t) = \left(\frac{\phi_p+\phi_2-\phi_1}{2}\right)$ implies that the $S(t)$ signal is equivalent to a beating at frequency ω_{beat}, $S(t) \propto \cos^2(\omega_{beat}\,t)$, where

$$\omega_{beat} = \frac{\partial\Delta\phi(t)}{\partial t} = \frac{\partial\omega}{\partial t}\frac{\partial\Delta\phi(t)}{\partial\omega} = \frac{\partial\omega}{\partial t}\left(\Delta L\frac{\partial k_g}{\partial\omega} - \int_L \frac{\partial k_p}{\partial\omega}dl\right) \quad (1)$$

where k_p is

$$k_\mathrm{p} = \frac{\omega}{c}N_\mathrm{p} = \frac{\omega}{c}\frac{1}{2}\left(\sqrt{1-\frac{\omega_p^2}{\omega(\omega-\omega_g)}} + \sqrt{1-\frac{\omega_p^2}{\omega(\omega+\omega_g)}}\right) \quad (2)$$

with $\omega_p^2 = \frac{n_e e^2}{m\epsilon_0}$, being n_e the plasma electron density and $\omega_g = eB/m$ the electron gyrofrequency. ω_{beat} is a function of the waveguide and plasma dispersion relations only: $\omega_{beat} = \omega_{beat}[\omega(k_g),\omega(k_p)]$. In principle, a proper sweep $\frac{\partial\omega}{\partial t}$ would counter-compensate the dispersion of the branch elements, thus fixing ω_{beat}. In the presence of the plasma chamber, acting as a resonator, we should rewrite the ω_{beat} expression such as $\omega_{beat} = \omega_{beat}[\omega(k_g),\omega(k_p),\omega(k_c)]$, i.e., including the dispersion relation $\omega(k_c)$ of the resonator itself. The latter is, unfortunately, a well-known collection of modes which results in a non-mathematical function. Hence we decided to use a linear ramp $\omega(t)$, i.e., $\partial\omega/\partial t = \mathrm{const.}$, then filtering out the cavity effects only in "*a posteriori*" analysis. Despite of any additional spurious components coming from the multi-paths into the cavity, the effect of the plasma is

a)Electronic mail: davidmascali@lns.infn.it.

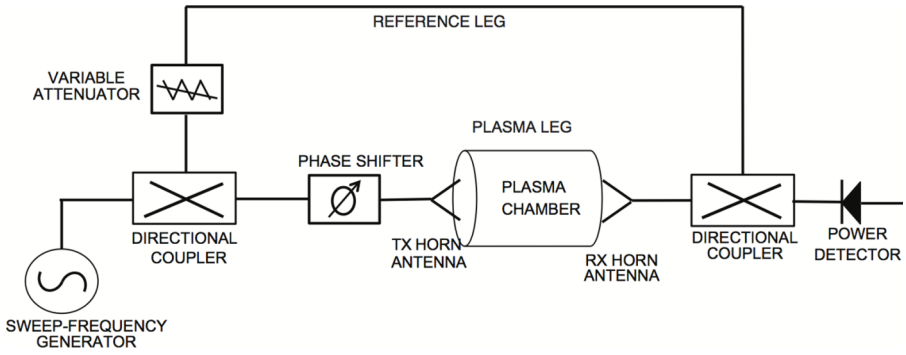

FIG. 1. Block diagram of the frequency-sweep interferometer VESPRI.

to shift the beating frequency due to the $\int_L \frac{\partial k_p}{\partial \omega} dl$ term. This $\Delta\omega_{beat}$ is therefore the physical observable we want to measure.

A. Calibration and measurements

The term $\Delta L \frac{\partial k_g}{\partial \omega}$ must be known with as high as possible accuracy, but the reference leg includes several microwave components such as the phase shifter, the attenuator, etc., which potentially introduce additive unknown terms of the same form. Since these terms remain the same with and without the plasma, an absolute calibration can be performed "*a priori*." Before calibration, in order to determine the beating due to the horn-to-horn signal only, the interferometer was operated in free-space, by placing the antennas at the same distance ($L = 30.2$ cm) as they would stand when mounted on the endplates of the plasma chamber. In this latter case, the antennas faced each other along a diagonal line of sight, in order to intercept the entire plasma volume and, especially, its core, as depicted in Figure 2. The chamber has length $L_c = 266$ mm and diameter $D = 120$ mm, and it is surrounded by a permanent magnet producing a quasi-flat magnetic field with maximum of 0.1 T.

The FFT on the beating signal in the empty cavity is allowed to extract the "in-cavity" beating frequency: $\omega_{beat_V} = 2\pi(0.3974)$ rad/s. The calibration was then performed by replacing the unknown term $\Delta L \frac{\partial k_g}{\partial \omega}$ in Equation (1) by a calibrating factor C_F such as

$$\omega_{beat_V} = \frac{\Delta\omega}{\Delta t}\left(C_F - \frac{L}{c}N\right) \tag{3}$$

with ω ranging from 18.5 to 26.5 GHz, $L = 30.2$ cm, and $\Delta t = 90$ s. Assuming $N = 1$ as vacuum refraction index, C_F was determined, then used for deriving the plasma refraction index N_p according to the relation

$$N_p = \frac{c}{L}\left[C_F \omega_b^{pl} - \frac{\Delta t}{\Delta \omega}\right]. \tag{4}$$

As an additional, intermediate step before probing the plasma, a bulk wax of paraffin (a material of well-known refraction index) was introduced into the plasma chamber, filling its entire volume. Finally, a $1.5 \cdot 10^{-4}$ mbar nitrogen plasma (0.1 T of maximum magnetic field) was sustained by 150 W of microwave power, at 3.75 GHz in off-resonance heating mode (see Ref. 4 for more details).

The temporal trends of the measured signals in the case of empty, paraffin, plasma filled cavity are shown in Fig. 3.

They are clearly different, thus confirming the method is sensitive to the different media introduced inside the cavity and especially to the plasma. The signals oscillate in the range of Hz, since any high frequency (GHz) beating was filtered out due to the intrinsic low-passband filtering of the RF diodes we used. The instrument was able to discriminate up to 10^{-3} Hz. It is worth noticing the much smoother signal detected in the case of the paraffin wax, probably due to a focusing effect which damps the multi-paths coming from the chamber walls. The

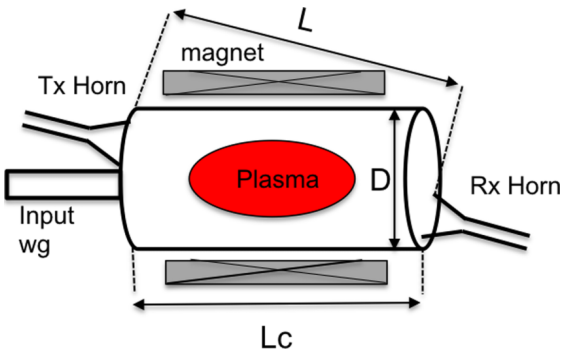

FIG. 2. Layout of the frequency-sweep interferometer VESPRI installed on the plasma reactor with oblique launching of the waves.

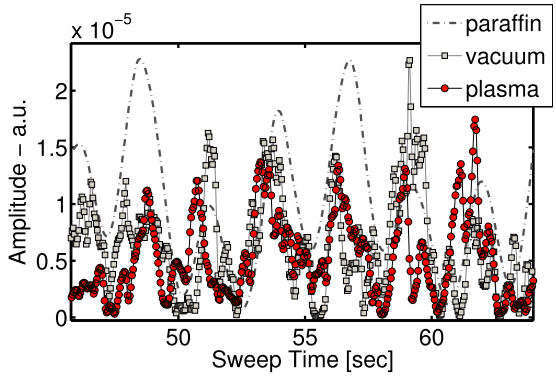

FIG. 3. Part of the sweeping time window for a comparison among the measured beatings in the case of empty, paraffin, or plasma filled cavity.

TABLE I. Horn-to-horn signal beating frequencies and corresponding indexes of refraction. Comparison among the three cases: empty, paraffin, and plasma filled cavity.

Medium	P_{RF} (W)	ω_{beat} (rad/s)	Refr. index N
Empty Cavity	0	$2\pi * 0.397$	1[a]
Bulk Paraffin	0	$2\pi * 0.380$	1.43[b]
Plasma	150	$2\pi * 0.407$	0.79 ± 0.11[c]

[a] Assumed by definition for the absolute calibration.
[b] In agreement with the literature value $N_{20\mathrm{GHz}} \simeq 1.45$.
[c] Error evaluation in a series of ten measurements.

FFT analysis allowed to evaluate the refraction indexes of the paraffin and, especially, of the plasma, as reported in Table I, thanks to the horn-to-horn beating frequency shift. The paraffin index of refraction resulted to be very close to the literature one. We then performed the sequence of measurements (while keeping constant the plasma parameters) shown in Figure 4, in order to estimate the statistical error for the plasma. The total relative error was around 14% with a less-than-one refraction index $N_p = 0.79$.

The final step was to determine the plasma density value. The adopted method can be summarized by the plot of Figure 5. The two curves in the figure depict the dispersion relation of the magnetoplasma (Eq. (2)) versus the plasma density n_e. They are plotted for the two frequencies f_1 = 18.5 GHz and f_2 = 26.5 GHz, f_1 and f_2 being the minimum and maximum frequencies of the sweep. We considered mainly the lower curve (the one obtained for f_1) , thus assuming that the plasma affected the propagation of the lower frequencies especially. The measured index $N_p = 0.79$ has its own error bar, which produces the horizontal dotted lines in the figure. The interception of such lines with the $N(n_e)$ curve determines, as a projection on the n_e axis, two values of n_e that were assumed as error bar, being the assumed line-integrated density along the line-of-sight $\overline{n}_e$ given by their averaged value, such as $\overline{n}_e = 2.1 \pm 1.0 \cdot 10^{18}$ m^{-3}.

A Langmuir probe, consisting of a 0.15×4 mm tungsten rod protruding from an alumina sheath of 37.5 cm in length, was used for comparative measurements. In order to avoid any influence by the strong external magneto-static field on the estimated density and temperature values (B-field especially affects the electronic charge collection), we analyzed the ion current part only of the recorded I-V curve. Different theoretical models were applied (such as orbital motion limited (OML), Lafambroise, Allen, Boyd and Reynolds

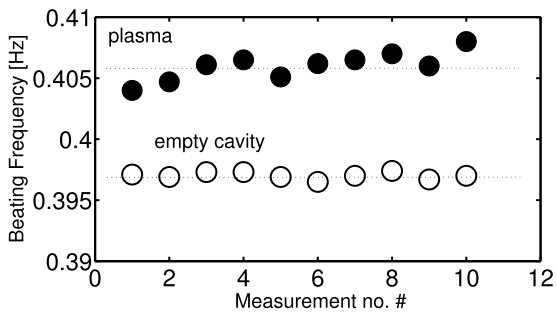

FIG. 4. Series of measurements of the beating frequency in the case of empty or plasma filled cavity, for the reproducibility check and error estimation.

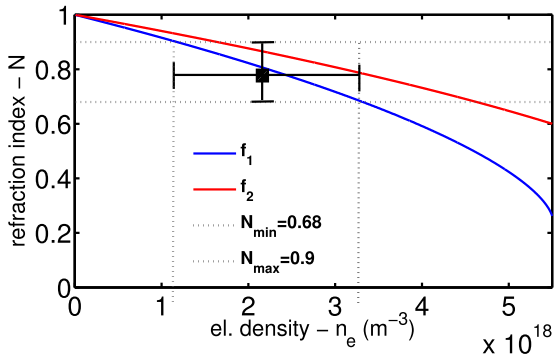

FIG. 5. Dispersion relation (Eq. (2)) at $f_1 = 18.5$ GHz and $f_2 = 26.5$ GHz (boundaries of the frequency range Δf) versus the electron density n_e. The square represents the argued value of n_e corresponding to the measured N_{pl}.

TABLE II. Plasma densities and relative errors measured by the interferometry or by a movable Langmuir Probe. The cutoff density at the corresponding frequency (3.7576 GHz) is given as reference.

	Density n_e (m^{-3})	Error	P_{RF} (W)
Interferometry[a]	$2.1 \cdot 10^{18}$	$\pm 1.0 \cdot 10^{18}$	150
Langmuir probe[b]	$5.5 \cdot 10^{17}$	$\pm 1.5 \cdot 10^{17}$	150
cutoff[c]	$1.2 \cdot 10^{17}$	...	...

[a] Line-averaged value.
[b] Line (of probe penetration)-averaged value.
[c] At the pumping wave frequency $f = 3.7576$ GHz.

(ABR), Bernstein–Rabinowitz–Laframboise (BRL), etc.) and compared with each other. Then, the error on the density evaluation was estimated from such a comparison. The Langmuir probe (LP) penetrated inside the plasma chamber from the side opposite to the endplate in which the waveguide for the pumping wave launching is placed. The measurements were done along the entire plasma chamber, at steps of 1 cm each. The data reported in Table II correspond to the average along the line of penetration. Differently from data reported in Ref. 3, this time the two collected values are rather different from each other: the one collected by the interferometry is almost four times larger than the Langmuir probes one. The discrepancy can be easily explained. We in fact performed CST-Microwave Studio simulations of the inner plasma chamber electromagnetic field with and without the Langmuir probe. The simulations showed that the probe, being a metallic coaxial cable surrounded by the alumina sheath, heavily perturbs the electromagnetic propagation inside the resonator, hence the plasma and the wave's propagation inside of it. It resulted in a higher reflected power, in a symmetry breaking of the TE or TM modes established in the cavity, in a less efficient modal conversion and, eventually, in a lower electron density value. Due to the fact that these small-size systems are inherently sensitive to electromagnetic perturbations of the plasma chamber, the collected data demonstrate how helpful will be the availability of non-intrusive diagnostics tools.

III. CONCLUSIONS

The frequency-sweep method has proved to be a powerful method for probing plasmas of compact ECR-type ion sources, where traditional interferometry techniques cannot

be applied. The measurements demonstrate that the absolute plasma density can be measured in a non-intrusive way; this will have the potentiality to improve the tuning of existing sources in terms of magnetic trapping and RF coupling, also helping in the design of high performance future machines.

ACKNOWLEDGMENTS

We wish to acknowledge the support of Santi Passarello and of the INFN-LNS mechanical workshop for the design and manufacture of several VESPRI items. This work was supported by the INFN 5th Nat. Comm.—Grant VESPRI.

[1]M. Heald and C. Wharton, *Plasma Diagnostics with Microwaves*, Wiley Series in Plasma Physics (Wiley, 1965).
[2]G. Torrisi, D. Mascal, L. Neri, O. Leonardi, G. Sorbello, L. Celona, G. Castro, R. Agnello, A. Caruso, S. Passarello, A. Longhitano, T. Isernia, and S. Gammino, Rev. Sci. Instrum. **87**, 02B909 (2016).
[3]E. E. Scime, R. F. Boivin, J. L. Kline, and M. M. Balkey, Rev. Sci. Instrum. **72**, 1672 (2000).
[4]D. Mascali, L. Celona, S. Gammino, R. Miracoli, G. Castro, N. Gambino, and G. Ciavola, Nucl. Instrum. Methods Phys. Res., Sect. A **653**, 11–16 (2011).